U.S. DEPARTMENT OF ENERGY

PNNL-18327

Prepared for the U.S. Department of Energy
under Contract DE-AC05-76RL01830

Estimate of the Distribution of Solids Within Mixed Hanford Double-Shell Tank AZ-101: Implications for AY-102

BE Wells
JJ Ressler

April 2009

Pacific Northwest
NATIONAL LABORATORY

DISCLAIMER

PACIFIC NORTHWEST NATIONAL LABORATORY
operated by
BATTELLE
for the
UNITED STATES DEPARTMENT OF ENERGY
under Contract DE-ACO5-76RL01830

Printed in the United States of America

Available to DOE and DOE contractors from the
Office of Scientific and Technical Information,
P.O. Box 62, Oak Ridge, TN 37831-0062;
ph: (865) 576-8401
fax: (865) 576 5728
email: reports@adonis.osti.gov

Available to the public from the National Technical Information Service,
U.S. Department of Commerce, 5285 Port Royal Rd., Springfield, VA 22161
ph: (800) 553-6847
fax: (703) 605-6900
email: orders@nits.fedworld.gov
online ordering: http://www.ntis.gov/ordering.htm

PNNL-18327

Estimate of the Distribution of Solids Within Mixed Hanford Double-Shell Tank AZ-101: Implications for AY-102

BE Wells
JJ Ressler

April 2009

Prepared for
the U.S. Department of Energy
under Contract DE-AC05-76RL01830

Pacific Northwest National Laboratory
Richland, Washington

Summary

This paper describes the current level of understanding of the suspension of solids in Hanford double-shell waste tanks while being mixed with the baseline configuration of two 300-horsepower mixer pumps. A mixer pump test conducted in Tank AZ-101 during fiscal year 2000 provided the basis for this understanding. Information gaps must be filled to demonstrate the capability of the baseline feed delivery system to effectively mix, sample, and deliver double-shell tank waste to the Hanford Tank Waste Treatment and Immobilization Plant (WTP) for vitrification.

Section 2 describes the distribution of solids in AZ-101 following mixer pump operation. The tank configuration and the best-estimate values of the waste properties during the test are described. It is concluded that the mixing in AZ-101 resulted in suspension of 32% of the particulate required for homogenous suspension. Section 3 describes the waste properties and tank configuration of Tank AY-102, which is the WTP commissioning feed tank. Section 4 compares the waste properties and tank configuration of the two tanks, and the results of the AZ-101 test are applied to AY-102. The comparison suggests that AY-102 will not be homogenously mixed by the baseline mixing system. The findings are also applied to Hanford waste in feed staging tanks in general, indicating that the baseline mixing system will face significant challenges in those tanks with regard to homogenous suspension of the Hanford insoluble solids. Finally, there are recommendations for future studies to reduce uncertainties in the homogeneity of mixed tank wastes.

Acronyms and Abbreviations

ALC	airlift circulator
DST	double-shell tank
PSDD	particle size and density distribution
SSP	Suspended Solids Profiler
TWINS	Tank Waste Information System (database)
UDS	undissolved solids
URSILLA	Ultrasonic Interface Level Analyzer
WTP	Hanford Tank Waste Treatment and Immobilization Plant

Contents

Figures

Tables

1.0 Introduction

The Hanford double-shell tank (DST) system provides the staging location for waste feed delivery to the Hanford Tank Waste Treatment and Immobilization Plant (WTP). Hall (2008) includes WTP acceptance criteria that describe physical and chemical characteristics of the waste that must be certified as acceptable before the waste is transferred from the DSTs to the WTP. The first stage of the DST Mixing and Sampling Demonstration Program is focused on defining the information gaps that must be filled to successfully demonstrate the capability of the baseline feed delivery concept to effectively mix, sample, and deliver DST waste to the WTP. Understanding the mixing performance of the baseline DST mixing systems is thus necessary to define the specific functional requirements of the DST sampling and feed transfer systems.

A significant amount of demonstration and computer modeling has been done at Hanford and Savannah River that focused on the effective cleaning radius of submerged pumps and their ability to mobilize waste solids off the bottom of the tank (Onishi and Wells 2004; Enderlin et al. 2003; Onishi et al. 2000; etc.). The rigorous characterization and acceptance requirements identified in ICD-19 dictate a more thorough understanding of the suspended slurry that results from mobilizing the solids off the tank bottom.

The objective of this work is to describe the current level of understanding of the suspension of solids in Hanford DSTs while being mixed with the baseline configuration of two 300-horsepower mixer pumps. The mixer pump test conducted in AZ-101 during fiscal year 2000 provided the basis of understanding (Carlson et al. 2001). In Section 2, the mixer pump operation in AZ-101 is summarized, the waste properties and tank configuration are presented, and the quantity of suspended solids resulting from the AZ-101 mixer pump tests relative to homogenous mixing is evaluated.

AY-102 is the WTP commissioning feed tank, and the solids suspension therein is thus considered via the solids suspension performance of the baseline feed delivery mixer pumps in AZ-101. The waste properties and tank configuration of AY-102 are presented in Section 3. The AZ-101 and AY-102 waste properties and tank configurations are compared in Section 4, and the suspension of solids in AY-102 and more broadly to the Hanford waste in general for other WTP DST feed staging tanks is estimated. Recommendations for improving the understanding of solids suspension during mixer pump operation are provided.

2.0 Distribution of Solids in AZ-101 Resulting from Mixer Pump Operation

The baseline configuration of two 300-horsepower mixer pumps was used to mobilize the sediment layer in AZ-101 during testing from 4/27/00 to 5/31/00 (Carlson et al. 2001). In Section 2.1, the AZ-101 waste properties and tank configuration are presented. The mixer pump operation and tank instrumentation pertinent to understanding solids suspension are summarized in Section 2.2, and solids suspension is evaluated in Section 2.3.

2.1 AZ-101 Waste Properties and Tank Configuration

Best-estimate values for AZ-101 waste properties at the time of the mixer pump test pertinent to the current evaluation have been determined based on the available data (Section 2.1.1). Given the different data sources, etc., significant digits are not considered, and all values are best-estimate approximations. The tank configuration is summarized in Section 2.1.2.

2.1.1 AZ-101 Waste Properties

The waste stored in AZ-101 before the mixer pump test consisted of a deep liquid layer overlaying a settled solids layer. The waste depth in AZ-101 was approximately 308 inches at the commencement of the mixer pump operations. Due to the failure of the pump column rupture disk in Mixer Pump 2, approximately 60,000 gallons of water were added during the operation of Mixer Pump 2, resulting in a final total waste depth of approximately 329 inches (Carlson et al. 2001). This water addition was approximately 7% by volume of the original liquid volume (supernate and interstitial liquid in the sediment, assumed to be synonymous).

2.1.1.1 AZ-101 Liquid and Undissolved Solids

The liquid density in AZ-101 at commencement of the mixer pump operations (subsequently referred to as the initial condition) was approximately 1.24 g/mL (TWINS[a]). Assuming that no solids dissolved, the water addition reduced the liquid density at the completion of the mixer pump operations (subsequently referred to as the final condition) to 1.22 g/mL (Hu 2007). The liquid temperature at the completion of the mixer pump operations was approximately 144°F (Carlson et al. 2001), and the dynamic viscosity of the AZ-101 liquid at that temperature was approximately 2 cP (Callaway 2000).

The density of the initial sediment (undissolved solids [UDS] and interstitial liquid) was 1.62 g/mL (Carlson et al. 2001). With a UDS density of 2.43 g/mL,[b] the UDS content in the sediment can be estimated at 32% by volume, 48% by mass via

---

(a) Core sample Data from TWINS: Tank Waste Information System database. http://twins.pnl.gov/twins3/twins.htm

(b) PNNL Letter Report to CH2M Hill: BE Wells. 2004. *Evaluation of Waste Data for Rheological Models Used in Waste Pipeline Transfer Assessment*. TWS05.001, Pacific Northwest National Laboratory, Richland, WA.

$$\phi_S = \frac{\rho_B - \rho_L}{\rho_S - \rho_L} \tag{2.1}$$

and

$$w_S = \phi_S \frac{\rho_S}{\rho_B} \tag{2.2}$$

respectively, where ρ_B, ρ_S, and ρ_L denote the bulk, UDS, and liquid densities.

The initial sediment depth, h_S, was approximately 17.5 inches.[(a)] Thus, the UDS mass in the tank is given by

$$m_{UDS} = h_S A_T \rho_B w_S \tag{2.3}$$

with A_T denoting the tank area, to be 141,565 kg. The initial and final liquid masses are 3,909,277 kg and 4,128,202 kg, respectively. A fully mixed condition in the tank at the end of the mixer pump test would thus have a UDS content of approximately 1.7% by volume, 3.3% by mass.

2.1.1.2 AZ-101 Undissolved Solids Particulate Characterization

The UDS particulate in AZ-101 can be characterized by a particle size and density distribution (PSDD). An AZ-101 PSDD was created according to the Case 3 approach of Wells et al. (2007). The Case 3 approach assigns the primary particulate density of the solid phase compounds (i.e., crystal density) to the particulate, independent of particle size. As such, solids particle density reduction (by agglomeration) below the primary crystal density is not accounted for. As discussed in Wells et al. (2007), this approach does not represent the actual phenomenon of Hanford particulate agglomeration, but it was selected because it provides an upper-bound for possible particle size and density, and it removes the significant uncertainty of quantifying the fractal dimension relating the agglomeration size and density. The presented PSDD developed using this approach is a representation of the AZ-101 UDS particulate. The discrepancy of the volume-weighted average UDS density from the PSDD of Table 2.1, 3.11 g/mL, and the UDS density in Section 2.1.1.1, 2.43 g/mL, is acknowledged.

The AZ-101 "minimal disturbance" PSD (Wells et al. 2007, Table A.4) was combined with the insoluble solid-phase compounds, volume fractions thereof, and crystal densities (Wells et al. 2007, Section 3.2). The resulting AZ-101 PSDD is provided in Table 2.1. Like the PSDDs of Wells et al. (2007), the AZ-101 PSDD in Table 2.1 is a 3-dimensional matrix of volume-based probability of each solid-phase compound in a particle-size distribution "bin" and its density in that bin. The PSDD bins represent the upper and lower size limit of the particles in each bin. For example, in Table 2.1, it can be seen that gibbsite [$Al(OH)_3$] comprises 75% of the solids particulate by volume, and gibbsite particles > 7.74 μm and less than or equal to 10 μm have a density of 2.42 g/mL and make up 3.6% of the solids by volume.

(a) Average of sludge weight data taken from publically released spreadsheet *SVF-1112 all solids R0.xls* provided via e-mail from JM Conner, CH2M Hill to BE Wells, PNNL, on 3/14/08.

Table 2.1. AZ-101 PSDD

Particle Size (μm)	Solid Phase Compounds and Density (g/mL)								
	$Al(OH)_3$ 2.42	Fe_2O_3 5.24	ZrO_2 5.68	$Ca_5OH(PO_4)_3$ 3.14	$Ni(OH)_2$ 4.1	$Na_2U_2O_7$ 5.617	MnO_2 5.026	$LaPO_4•2H_2O$ 6.51	PuO_2 11.43
	Solid Volume Fraction								
0.22	3.8E-04	7.7E-05	2.4E-05	6.9E-06	6.7E-06	4.9E-06	1.1E-06	3.7E-06	2.5E-08
0.28	9.1E-03	1.9E-03	5.7E-04	1.7E-04	1.6E-04	1.2E-04	2.7E-05	9.0E-05	6.0E-07
0.36	1.0E-02	2.1E-03	6.4E-04	1.9E-04	1.8E-04	1.3E-04	3.1E-05	1.0E-04	6.8E-07
0.46	1.3E-02	2.7E-03	8.4E-04	2.5E-04	2.4E-04	1.7E-04	4.0E-05	1.3E-04	8.8E-07
0.60	1.8E-02	3.6E-03	1.1E-03	3.2E-04	3.1E-04	2.3E-04	5.3E-05	1.7E-04	1.2E-06
0.77	2.2E-02	4.5E-03	1.4E-03	4.0E-04	3.9E-04	2.9E-04	6.5E-05	2.2E-04	1.4E-06
1.00	5.4E-02	1.1E-02	3.4E-03	9.9E-04	9.6E-04	7.0E-04	1.6E-04	5.3E-04	3.6E-06
1.29	5.1E-02	1.0E-02	3.2E-03	9.3E-04	9.0E-04	6.6E-04	1.5E-04	5.0E-04	3.4E-06
1.67	4.6E-02	9.4E-03	2.9E-03	8.5E-04	8.2E-04	6.0E-04	1.4E-04	4.6E-04	3.0E-06
2.15	6.1E-02	1.2E-02	3.8E-03	1.1E-03	1.1E-03	7.9E-04	1.8E-04	6.0E-04	4.0E-06
2.78	5.6E-02	1.1E-02	3.5E-03	1.0E-03	1.0E-03	7.3E-04	1.7E-04	5.6E-04	3.7E-06
3.59	6.0E-02	1.2E-02	3.8E-03	1.1E-03	1.1E-03	7.9E-04	1.8E-04	6.0E-04	4.0E-06
4.64	6.8E-02	1.4E-02	4.3E-03	1.3E-03	1.2E-03	8.9E-04	2.0E-04	6.8E-04	4.5E-06
5.99	6.2E-02	1.3E-02	3.9E-03	1.1E-03	1.1E-03	8.1E-04	1.8E-04	6.1E-04	4.1E-06
7.74	6.3E-02	1.3E-02	4.0E-03	1.2E-03	1.1E-03	8.3E-04	1.9E-04	6.3E-04	4.2E-06
10.00	3.6E-02	7.3E-03	2.2E-03	6.6E-04	6.3E-04	4.7E-04	1.1E-04	3.5E-04	2.4E-06
12.92	3.5E-02	7.2E-03	2.2E-03	6.5E-04	6.2E-04	4.6E-04	1.0E-04	3.5E-04	2.3E-06
16.68	3.2E-02	6.6E-03	2.0E-03	6.0E-04	5.8E-04	4.2E-04	9.7E-05	3.2E-04	2.1E-06
21.54	2.8E-02	5.7E-03	1.8E-03	5.2E-04	5.0E-04	3.7E-04	8.4E-05	2.8E-04	1.8E-06
27.83	2.3E-02	4.7E-03	1.5E-03	4.3E-04	4.1E-04	3.0E-04	6.9E-05	2.3E-04	1.5E-06
35.94	4.7E-03	9.5E-04	2.9E-04	8.6E-05	8.3E-05	6.1E-05	1.4E-05	4.6E-05	3.1E-07
Total Solid-Phase Volume Fraction	0.75	0.15	0.047	0.014	0.013	0.010	0.002	0.007	0.00005

The particle sizes and densities of the AZ-101 PSDD can be used in the settling velocity equation from Camenen (2008)

$$U_T = \frac{\nu}{d}\left(\sqrt{15+\sqrt{Ga/0.3}}-\sqrt{15}\right)^2 \tag{2.4}$$

where Ga is the Galileo number defined by

$$Ga = \frac{\left(\frac{\rho_S}{\rho_L}-1\right)gd^3}{\nu^2}, \tag{2.5}$$

where ν is the kinematic viscosity of the fluid, and d is the particle diameter.

The cumulative volume-based probability of the settling velocity of the AZ-101 insoluble solids, shown in Figure 2.1, is created using the settling velocities (Equation [2.4]) and volume fractions of Table 2.1. In Figure 2.1, the 50th percentile (median) and 95th percentile by volume of settling velocity are approximately 6.4E-6 and 2.3E-4 m/s, respectively.

Comparing the initial *in situ* settling velocity of the solid-liquid interface during the settling test at the completion of the mixer pump test (see Section 2.2) from Carlson et al. (2001), approximately 6E-4 m/s, to the AZ-101 PSDD settling velocity of Figure 2.1 indicates that the *in situ* settling rate is greater than the 99th percentile by volume of the PSDD settling velocity. This comparison, indicating that for *in situ* settling in AZ-101, the trailing edge of the solid-liquid interface (i.e., the slowest settling particulate) settles at the rate of the fastest settling particulate, was not expected.

A plausible solid-liquid interface settling velocity for homogenously suspended particulate can be obtained using the volume-weighted average settling velocity, defined by

$$\overline{U} = \frac{\sum_{i=1}^{n} x_i U_i}{\sum_{i=1}^{n} x_i} \tag{2.6}$$

where x_i is the volume fraction of solid i relative to the total solid volume, U_i is the settling velocity (Equation 2.4), and n is the number of entries in the PSDD (i.e., the number of particle-size bins multiplied by the number of solid-phase compounds).[(a)]

The volume-weighted average settling velocity of the AZ-101 PSDD (Table 2.1) is 4.3E-5, which is 7% of the *in situ* interface settling velocity of 6E-4 m/s. With regards to whether the AZ-101 particulate was homogenously suspended, it is pertinent to consider that the suspension was due to mixer pump

(a) To provide a representative volume-weighted average, a minimum i, dependent on the primary distribution, is required.

operation. It is reasonable to assume that, if some of the initial sediment was not suspended (see Section 2.3), the UDS particulate that was suspended would have been the "lighter" material, i.e., the particulate with low settling velocities. Thus, the apparent discrepancy between the *in situ* and PSDD-based settling velocity may be even more pronounced than indicated by the comparison above.

These results from comparing settling velocities, given that the density of the particulate represented in the PSDD is conservatively high (see above), may imply that the particle sizes are biased low. Regardless, because the PSDD is defined as representative, and the PSDD for AY-102 is developed synonymously (Section 3), the AZ-101 and AY-102 waste characteristics were compared with the PSDDs as presented.

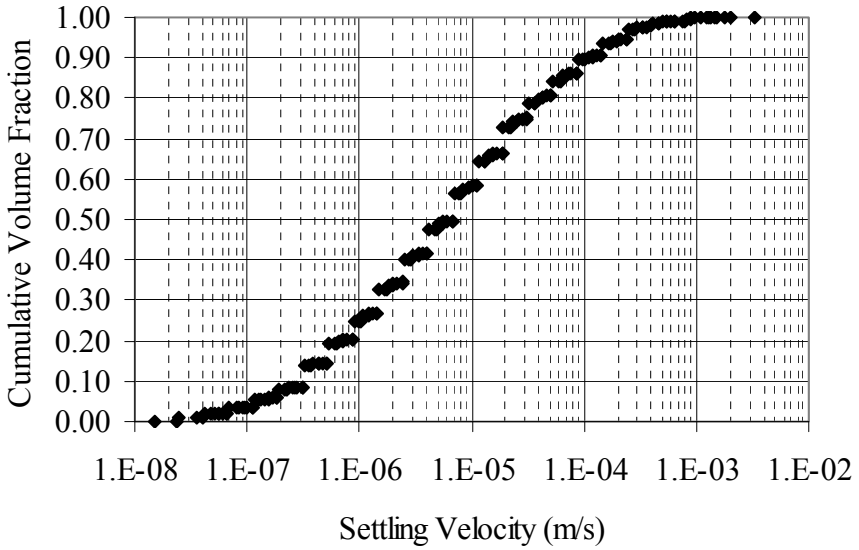

Figure 2.1. Cumulative UDS Volume Fraction as Function of Settling Velocity for AZ-101

2.1.2 AZ-101 Tank Configuration

Tank AZ-101 is a 37.5-ft radius 1,406,400-gallon DST with a maximum operating capacity of 1,159,600 gallons (Barker 2003). The fill level at the maximum operating capacity is approximately 421 inches.

Aside from multi-instrument trees, etc., the internal tank structures with the most potential to impact UDS mobilization and suspension during mixer pump operation are the 22 airlift circulators (ALCs) that were intended to mix the waste by introducing a stream of air bubbles into 30-inch-diameter cylindrical tubes with a bottom elevation 30 inches above the tank bottom (Stewart et al. 2005). Fifteen of the ALCs extend to 294 inches above the tank bottom, and the remainder to 234 inches. One ALC is located at the center of the tank, 7 ALCs are equally spaced along the circumference at a radius at 14.5 feet from the tank center, and the remaining 14 are equally spaced along the circumference at a radius at 27 feet.

2.2 Summary of AZ-101 Mixer Pump Operation

Two 300-horsepower Lawrence mixer pumps are installed in risers 1C (mixer pump 1) and 1A (mixer pump 2), see Figure 2.2. The mixer pumps take fluid in from 12 inches above the tank bottom and discharge it horizontally from two opposed 6-inch-diameter nozzles at 18 inches above the tank bottom.

Starting on 4/27/2000, mixer pump 1 was initially operated with the horizontal nozzle discharge at five fixed radial directions through a series of tests typically incrementally increasing in pump discharge speeds of nominally 725, 1,000, and 1,150 rpm. The pump was operated at each speed for approximately 3 hours. These rates approximately correspond to 7,100, 9,200, and 10,500 gpm total flow, or 12.3, 15.9, and 18.2 m/s for each nozzle.

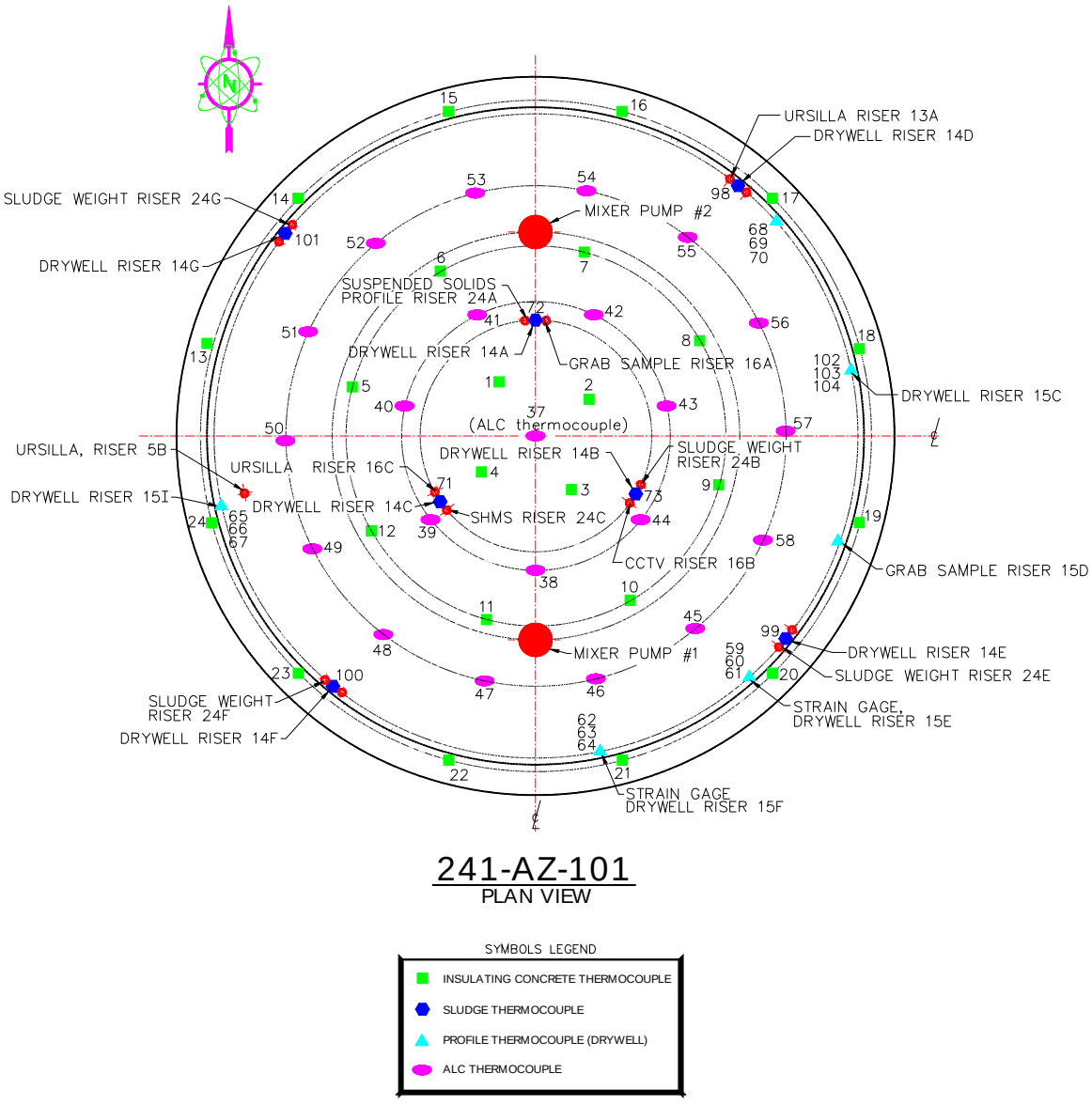

Figure 2.2. AZ-101 Instrumentation. Figure 3-4, Carlson et al. (2001).

Mixer pump 1 was then operated in oscillation mode (horizontal nozzle discharge, 180º pump rotation at 0.05 and 0.2 rpm) at each of the three nominal velocities totaling an operating period of almost 3.5 days. Mixer pumps 1 and 2 subsequently operated at equivalent rates, again ramping up at nominally 725, 1,000, and 1,150 rpm over a total operating period of approximately 11 days.

The total flow for both mixer pumps during the test was nominally 285.5 million gallons, which is equivalent to 336 final AZ-101 waste volumes. The final operation of the mixer pumps, consisting of concurrent oscillatory operation (0.05 rpm) for about 2.5 days at approximately 18 m/s, resulted in the re-circulation of 72 waste volumes through the mixer pumps. In this final operation, completed on 5/31/2000, mixer pump 1 was stopped at 12:51 PM because of operational issues, and mixer pump 2 was shut down at 4:20 PM.

Thermocouples located throughout the waste and in the tank floor indicate that 95 to 100% of the sediment was mobilized (Carlson et al. 2001). The time period immediately following the final operation of the mixer pumps is called the "settling test."

2.3 Suspended Solids Distribution in AZ-101

As reported in Section 2.2, 95 to 100% of the AZ-101 sediment was mobilized during the final mixer pump operation. The quantity of those mobilized solids that were suspended off the tank bottom by that operation is analyzed in this section.

The tank instrumentation, emphasizing those instruments pertinent to determining the UDS mobilization and suspension, is summarized in Section 2.3.1. The UDS distribution analysis and results are presented in Section 2.3.2.

2.3.1 AZ-101 Instrumentation Summary

AZ-101 mixer pump test instrumentation pertinent to the sediment mobilization and UDS suspension includes:

- Thermocouples (a thermocouple initially in the sediment is at a higher temperature than the supernate until the sediment at that location is mobilized)
- Ultrasonic Interface Level Analyzer (URSILLA) (uses ultrasonic ranging technique to measure vertical location of solid-liquid interface)
- Suspended Solids Profiler (SSP) (uses light reflectance to determine turbidity)
- Gamma-monitoring systems (detect radionuclides for concentration information)
- Grab samples (retrieved waste samples, analyzed for solid content, etc.)
- Sludge weights (essentially a metal weight on a tape measure, routinely used at Hanford to measure the solids level).

This instrumentation is located in AZ-101 as shown in the plan view tank diagram of Figure 2.2. The gamma-monitoring system was deployable in the drywell risers 14B, 15C, 15E, and 15F. Nine grab-sample "events," consisting of eight 125-mL grab samples taken incrementally throughout the waste depth, were obtained during testing. Grab-sample Events 5 through 9 were conducted after the final

mixer pump operation. Grab-sample Event 6 was taken from riser 15D, and all other grab-sample events were taken in riser 16A.

The thermocouple data were used to quantify the extent of the solids mobilization. The URSILLA, grab-sample, and gamma data establish the solid-liquid interface settling rate data (see Section 2.1.1.2) with very good agreement between the instruments (Carlson et al. 2001). Carlson et al. (2001) report that although the available SSP data are consistent with respect to the solid-liquid interface of the URSILLA and grab-sample data, insufficient data are available to correlate the SSP data to solids concentration.

With the exception of the thermocouples, which had data recorded at 1-minute intervals throughout the testing, none of the above-listed instrumentation was operated during mixer pump operation. The gamma-monitoring system, grab-samples events, and sludge weight data evaluated for the quantity of UDS suspension reported in Section 2.3.2. Thus, these values represent the UDS suspension immediately following mixer pump operation.

2.3.2 AZ-101 Suspended UDS Distribution

The AZ-101 mixer pump test data, specifically those from the settling test (see Sections 2.2 and 2.3.1), were evaluated for the quantity of UDS suspension. The approach to correlating the UDS concentration to the gamma count is similar to that reported in Carlson et al. (2001).[(a)] The current analysis develops the data set further as described in Section 2.3.2.1. The analysis approach was developed, and results are discussed in Section 2.3.2.2.

2.3.2.1 Data Set

The data set for quantifying the UDS concentration and gamma count from the AZ-101 mixer pump test is primarily based upon the analysis of the grab-sample event. The initial sediment condition is also considered.

Although gamma activity (counts per second, cps) data are available from two different instruments, Cart A and Cart B, only those data from Cart A were considered because only Cart A data were available for the settling test. Cart A was deployed in riser 15F during the first mixer pump operations and 15C for the remainder of the testing (see Figure 2.2 for riser location). Gamma profiles from Cart A in riser 15C taken during the settling test immediately following the final mixer pump operation are provided in Figure 2.3. The gamma monitoring was analyzed such that the count rate (cps) increase with higher UDS concentration (Carlson et al. 2001). Profile (1) of Figure 2.3, taken during the settling test from 0 to 73 minutes after cessation of mixer pump operation, shows a relatively uniform counting rate from approximately 38 to 290 inches, indicating a uniform distribution of solids. The data of Figure 2.3 are provided in tabular form Appendix A. Also included are data from pre-mixer pump conditions and those gamma scans with sufficient data to be associable with grab-sample Event 8.

Grab-sample Events 5 through 7 were taken at similar elevations in the tank and during the same time period as Profiles (1) through (5) of Figure 2.3. The grab-sample analysis data from Event 5 summarized in Carlson et al. (2001) were taken from Bell (2001). No chemical or radiochemical analyses were

---

(a) PJ Certa, September 13, 2001. *241-AZ-101 Mixer Pump Test Solids Profiles*. CH2M HILL Interoffice Memo, 7G300-01-DJW-008. CH2M HILL Hanford Group Inc., Richland, WA.

performed on the samples from Event 6 (Bell 2000), nor for Events 7 and 9 (Bell 2001). Data for analyzed samples from Events 5 and 8 that contained appreciable solids (equal to or greater than 0.766 g/L, Carlson et al. 2001) are provided in Table 2.2. The mass fraction of solids in the grab sample, w_{SG}, was computed from

$$w_{SG} = \left(1 - \frac{1 - w_{SCS}}{w_{HCL}}\right)\frac{V_{CS}}{V_B} \tag{2.7}$$

where w_{SCS} and w_{HCL} are the mass fraction of solids in the centrifuged solids and water in the centrifuged liquid, respectively, V_{CS} is the volume of centrifuged solids, and V_B is the bulk grab-sample volume. Figure 2.4 shows the time and elevation of the concurrent grab samples and gamma scans during the settling test.

Table 2.2. Grab-Sample Data

	Bell (2001)							Eqn. (2.7)
Sample Number	Date	Time	Elevation (in.)[(a)]	w_{SCS}	w_{HCL}	V_{CS} (mL)	V_B (mL)	w_{SG}
1AZ-00-35	5/31/00	16:31	6	0.545	0.6998	5.86	123.4	0.017
1AZ-00-36	5/31/00	16:40	48	0.512	0.713	5.08	128.2	0.013
1AZ-00-37	5/31/00	17:04	90	0.513	0.7162	5.01	130.5	0.012
1AZ-00-38	5/31/00	17:16	132	0.575	0.7051	3.22	92.24	0.009[(b)]
1AZ-00-39	5/31/00	17:41	174	0.516	0.708	3.2	125	0.008
1AZ-00-40	5/31/00	18:04	216	0.559	0.7087	0.2	128.2	0.001
1AZ-00-67	6/1/00	17:12	6	0.52	0.7054	35.09	118.8	0.094

(a) Elevation from Carlson et al. (2001).

(b) Approximately $^1/_3$ of the sample liquid was spilled and lost before analysis (Carlson et al. 2001). The presented result is "corrected" for liquid loss.

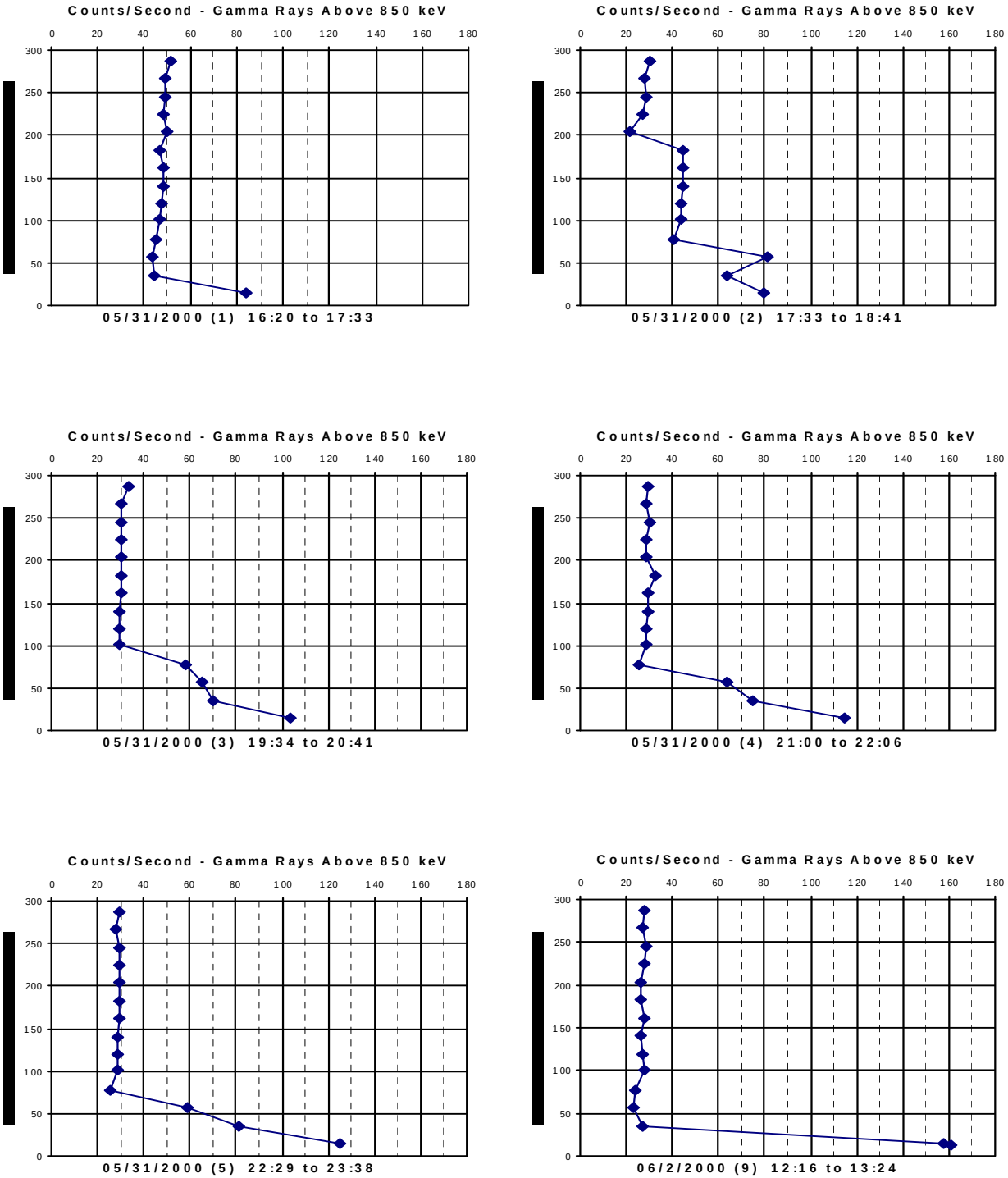

Figure 2.3. Gamma-Monitoring System Data from Cart A, Riser 15C, Settling Test Period, 0 to 45 Hours after Pump Shutdown (Figure 5-22, Carlson et al. 2001; Ordinate is Height Above Tank Bottom [inches])

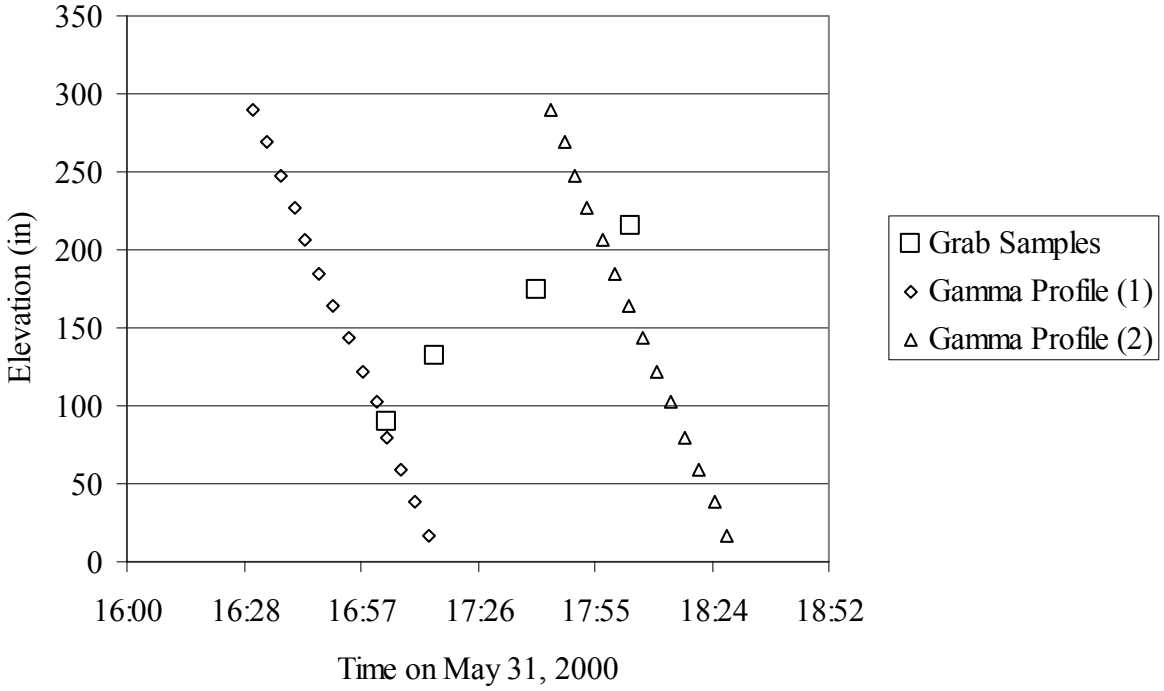

Figure 2.4. Grab-Sample and Gamma Monitoring System Data Concurrent in Time. Gamma Profile Numbers Correspond to Figure 2.3.

Using the mass fractions of water in centrifuged solids and liquids to determine the UDS density has been shown to over-predict the chemically plausible density (Onishi et al. 2002 and TWS05.001[(a)]). These results may suggest that the UDS content of the grab samples of Table 2.2 (synonymous with Bell 2001) are biased low.

Comparison of the UDS density computed via

$$\rho_S = \frac{\rho_B\left(1 - \frac{1 - w_{SCS}}{w_{HCL}}\right)}{1 - \frac{\rho_B}{\rho_L}\left(\frac{1 - w_{SCS}}{w_{HCL}}\right)} \tag{2.8}$$

from the data of Table 2.2 and Bell (2001) to the UDS density of 2.43 g/mL, given in Section 2.1, indicates that the mass fraction of solids in the grab samples may be 7 to 35% low depending on which sample is considered. Given the lack of definitive data, there was no attempt in the current analysis to reconcile potential differences, and the data of Table 2.2 were used as reported.

(a) PNNL Letter Report to CH2M Hill: Wells BE. 2004. *Evaluation of Waste Data for Rheological Models Used in Waste Pipeline Transfer Assessment*. TWS05.001, Pacific Northwest National Laboratory, Richland, WA.

By interpolating in elevation and time, concurrent solids-content information from the grab samples, Table 2.2, and the gamma data, Appendix A, as illustrated in Figure 2.4 can be developed, Table 2.3. Grab-sample data from 1AZ-00-35 and 1AZ-00-36 cannot be correlated with gamma cps, given the disparity in time, and, for the 6-inch sample, the elevation, Figure 2.4. The data for sample 1AZ-00-67 have the same elevation issue. All other data of Table 2.2 were considered.

In Table 2.3, data points 1 and 2 are from pre-mixer pump conditions on 4/27/00 and 4/31/00. The median gamma activity for the supernatant liquid ($w_S = 0$) is the median of the pre-mixer pump data above the initial sediment height. The gamma activity for the UDS content in the sediment, $w_S = 0.48$, Section 2.1.1.1, is the median of the data at 16 inches elevation. The latter data point is subject to relatively significant uncertainty given that the solids content is the average throughout the sediment, and the gamma datum is from essentially the very top of the sediment.

The post-test supernatant liquid cps, data point 3, is the median of the 6/2/00 data 38 inches in elevation and above. The solid-liquid interface data of the URSILLA, grab-sample, and gamma data indicate that this measurement does not include solids (Section 2.3.1). The change in liquid gamma activity from the pre-test condition to the settling test condition is attributed to the water addition over the test period (Section 2.1.1).

The gamma activity for data points 4 and 7 are liner interpolations in elevation only. For example, for data point 7, the gamma activity at approximately 17:02 and 17:04, 5/31/00 (Profile 1 of Figure 2.3 and Figure 2.4), from approximate elevations of 103 and 80 inches, respectively, was interpolated to the 90-inch elevation of sample 1AZ-00-37 of grab-sample Event 5, taken at 17:04 (see Figure 2.4).

Data points 5 and 6 were determined from the grab-sample data and linear interpolation of the gamma activity with elevation and then time to that of the pertinent grab sample. For data point 5, it can be observed from Figure 2.4 that sample 1AZ-00-39 (174 inches elevation at 17:41) is bounded in elevation and time by gamma Profiles 1 and 2 of Figure 2.3. Linear interpolation with the elevation between the gamma activity at 164 and 185 inches to 174 inches provides 48 cps at an average time of 16:49 and 44 cps at an average time of 18:01. Interpolation to 17:41 results in 45 cps. Data point 6 was developed similarly.

Table 2.3. UDS Content and Gamma Count Rate

Test Condition	Data Point Number	w_S	Gamma (cps)	UDS Gamma[(a)] (cps)
Pre-Test	1	0.0	34	0
	2	0.48	300	266
Settling Test	3	0.0	27	0
	4	0.001	31	4
	5	0.008	45	18
	6	0.009	47	20
	7	0.012	46	19

(a) The UDS gamma count has the contribution of the liquid for the applicable test condition removed.

2.3.2.2 Data Analysis and Discussion

The data of Table 2.3 were used to correlate the UDS concentration to the gamma count rate. As indicated in Carlson et al. (2001), the functionality of the response in gamma activity to solids concentration is unknown. Linear functionalities are presented and compared to an approximated radiation detection approach.

The data from the initial period of the settling test used to develop the data of Table 2.3 was the period of specific interest (see Section 2.3.1; no data were available during mixing, and thus the settling test data were evaluated). Thus, the exact functionality of the relationship is not as critical to the accuracy of the results; no extrapolation is required. The uncertainty of the data themselves, not the functionality of the relation, may therefore be expected to have the most significant impact on the accuracy of the results.

Two regions of Table 2.3 data were fit using linear least-squares regression. "Approach 1" developed fits for data points 2 through 7, while "Approach 2" used data points 3 through 7. Approach 2 exclusively uses the grab-sample data. The fits for each approach are shown in Figure 2.5. The relative fit for the grab-sample data points is highlighted in Figure 2.6 (close-up of Figure 2.5). The two different approaches were developed given the uncertainty of data point 2 as described above. The data of 0 cps, $w_S = 0$, is physical. Thus, fits with the intercept set to zero are also included in Figure 2.5 and Figure 2.6. For Approach 2, the grab-sample data, the difference is negligible.

The fits for Approach 1 over-predict the grab-sample mass fraction data by factors of approximately 2 to 3.5. Given the intended application as described above and the poor fit to the grab-sample data, the Approach 1 fits may not be appropriate. Conversely, Approach 2 is shown to significantly under-predict the estimated solids concentration for data point 2. The validity of inclusion or exclusion of data point 2 was evaluated with a mass balance of the UDS in the tank following comparison of the 0-intercept linear fits to that from the radiation-detection approach.

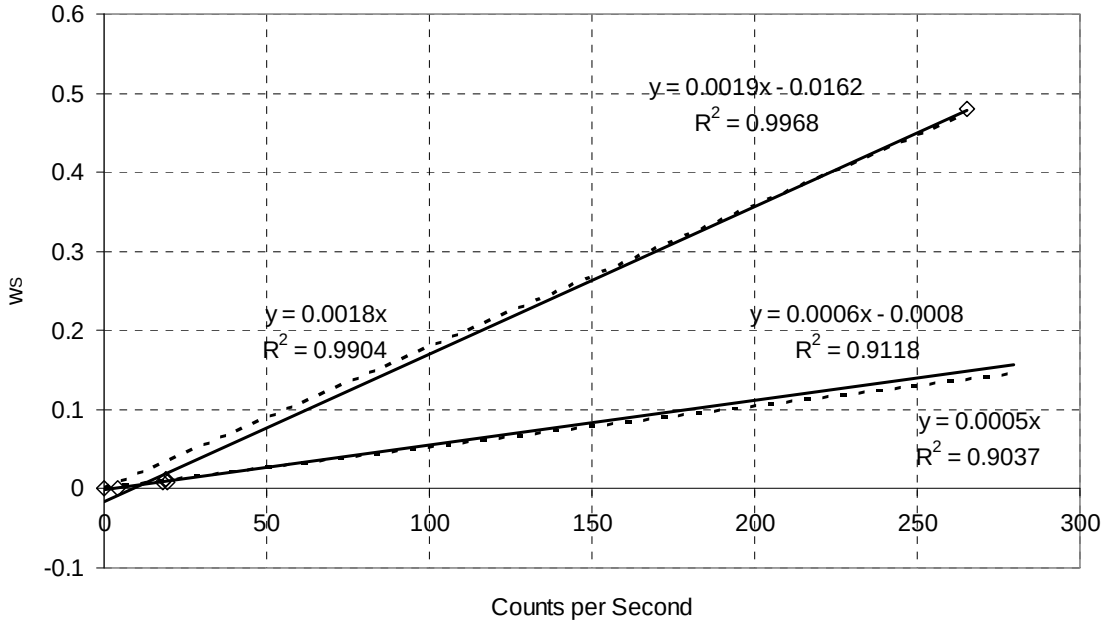

Figure 2.5. Mass Fraction of UDS, w_S, as a Function of Gamma Count

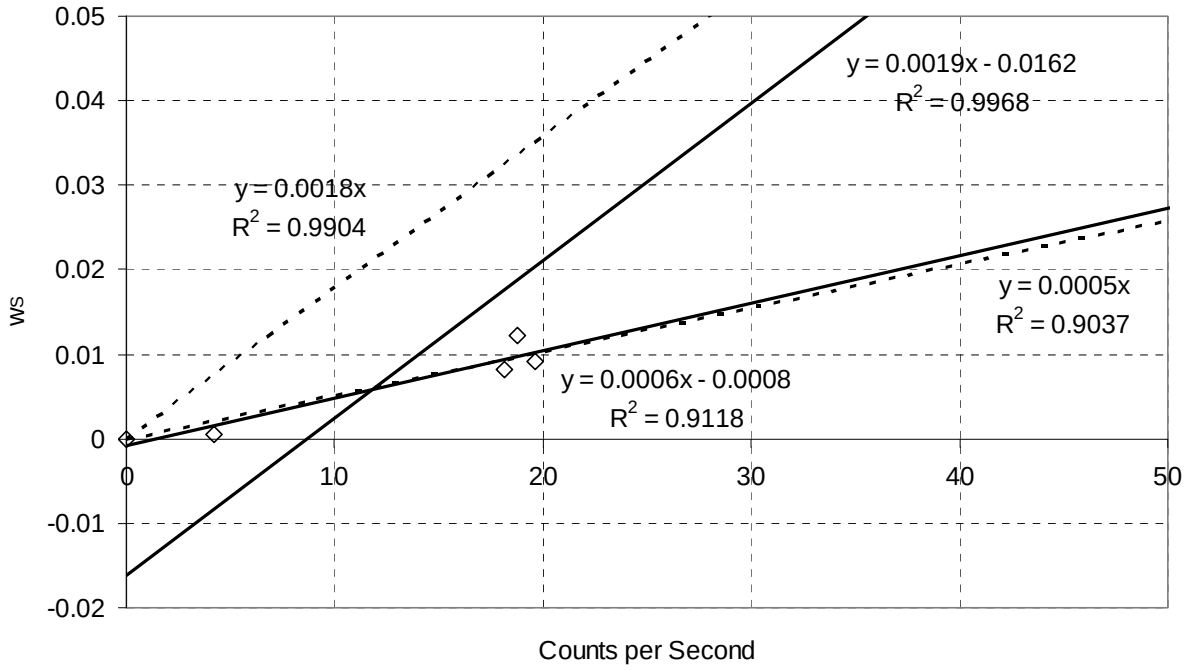

Figure 2.6. Mass Fraction of UDS, w_S, as a Function of Gamma Count (close up)

Synonymous with the 0-intercept linear fits of Approaches 1 and 2, it can be assumed that for a higher concentration of radioactive solids, the activity (cps) linearly increases. The activity emitted by a radioactive solid, A_{emit}, and observed, A_{obs}, may thus be expressed as

$$A_{obs} = A_{emit} = \lambda N_{rad} \tag{2.9}$$

where λ is the decay constant, and N_{rad} is the number of radioactive atoms (Knoll 2000). With the mass of the UDS, m_S, given by

$$m_S \equiv N_{rad} \frac{A_{rad}}{N_A} \frac{m_S}{m_{Srad}} \tag{2.10}$$

where A_{rad} is the mass (amu) of the radioactive solid, N_A is Avogadro's number, and m_{Srad} is the mass of the radioactive solid. Equation (2.9) can then be written as

$$A_{obs} = A_{emit} = Cm_S \tag{2.11}$$

where C is a constant. The mass of solids is $m_S = w_S m_B$; m_B is the total mass of solid and liquid. Thus, Equation (2.11) can be written in terms of the mass fraction of solids as

$$A_{obs} = A_{emit} = kw_S \tag{2.12}$$

where k is a constant.

It is expected that with more solids, there will be a higher probability for self-absorption. This phenomenon is approximated by considering that the transmission, T, can be expressed as

$$T = e^{-\frac{\mu}{\rho_B}\rho_B t} \tag{2.13}$$

where μ is the linear attenuation coefficient, and t is the thickness of the absorbing material (Knoll 2000). If it is assumed that $\mu = c\ \rho_B$ (c is a constant), the summation of the transmission from the radioactive solids over the maximum range of the detector, t_{max}, may be expressed as

$$T = \int_0^{t_{max}} e^{-a\rho_B t} dt = \frac{1}{a\rho_B}\left(1 - e^{-a\rho_B t_{max}}\right) \tag{2.14}$$

Then

$$A_{obs} = A_{emit} T \tag{2.15}$$

With Equation (2.12),

$$A_{obs} = k w_S \frac{1}{a\rho_B}\left(1 - e^{-a\rho_B t_{max}}\right) \tag{2.16}$$

The gamma probe was deployed in the center of drywells, which have a diameter of 6 inches (0.1524 m).[(a)] As t_{max} is un-physically decreased to less than 0.0762 m (distance from probe to drywell wall), the best fit of Equation (2.16) approaches the 0-intercept linear function for both Approaches 1 and 2. The fit with t_{max} set to the unphysical limit of the tank diameter, 22.86 m, is essentially equivalent to that with t_{max} set to 0.0762 m. Thus, t_{max} is approximated at 0.0762 m.

Equation (2.16) was fit to the data of Approaches 1 and 2 via a least-squares regression optimizing the predicted to the measured cps by adjusting constants k and a. The resultant fits are provided in Figure 2.7.

Given that there is minimal difference in the Equation (2.16) fits to the 0-intercept linear fits, significant approximating assumptions are required to achieve Equation (2.16), and a solution for w_S from Equation (2.16) is challenging [$\rho_B = f(w_S, \rho_S, \rho_L)$]; see Equation (2.20)[(b)]—the 0-intercept linear fits are analyzed further.

(a) *Tank AZ-101 Drywell Temperature Probe Assy & Install*, Drawing Number H-2-79229, Rev. 1.

(b) It is noted that the Lambert W function can be used to solve Equation (2.16) for w_S.

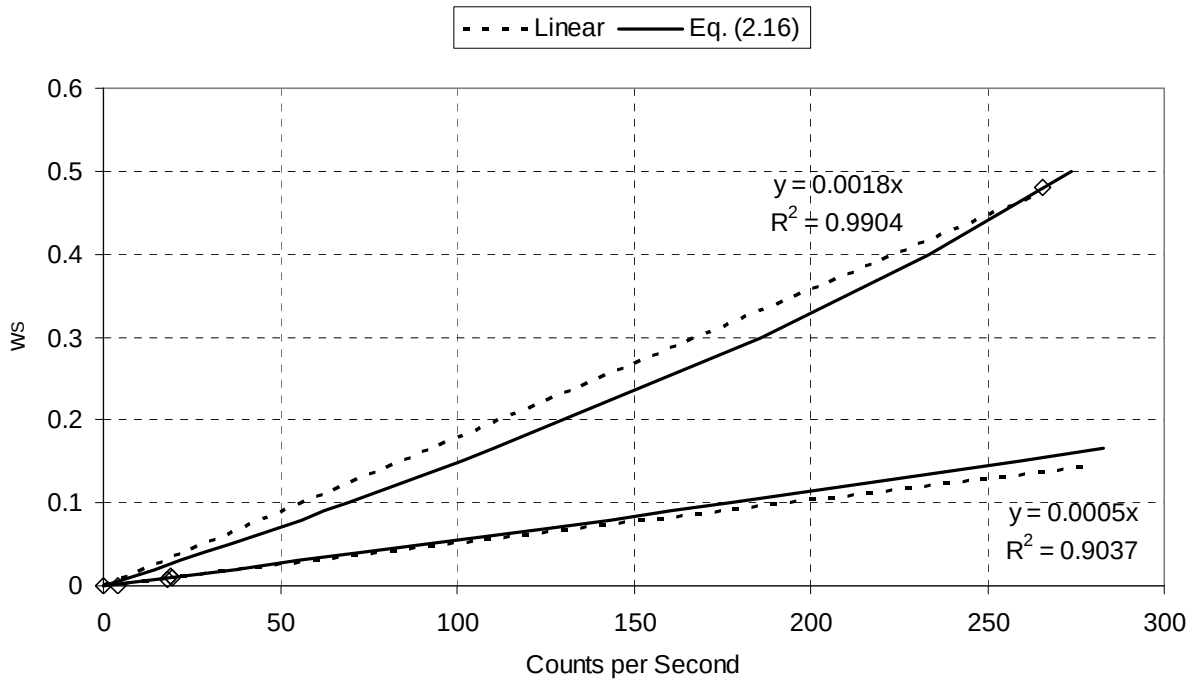

Figure 2.7. Mass Fraction of UDS, w_S, as a Function of Gamma Count, Comparison of 0-Intercept Linear and Equation (2.16)

The mass fraction results of the application of the Approach 1 0-intercept linear fit

$$w_S = 0.0018\text{cps} \tag{2.17}$$

and the Approach 2 0-intercept linear fit

$$w_S = 0.0005\text{cps} \tag{2.18}$$

to selected gamma scan data from Appendix A (liquid condition, 27 cps, data point 3, Table 2.3, subtracted from each reading) are provided in Table 2.4 and Table 2.5, respectively. As expected, comparing the predicted w_S to the measured w_S for data points 4, 5, 6, and 7 of Table 2.3 shows that Approach 1 over-predicts by factors of up to 6. Approach 1 also indicates solids loadings, albeit very low, at elevations the URSILLA and grab samples indicated were solids free.

Table 2.4. Mass Fraction of UDS from Gamma Count, Approach 1, Equation (2.17)

Elevation (in.)	w_S, Gamma Scan Identification # (see App. A, 5/31/00 to 6/2/00)							
	5	6	7	8	9	10	11	12
290	0.043	0.006	0.012	0.004	0.004	0.004	0.001	0.002
269	0.040	0.002	0.006	0.003	0.002	0.000	0.000	0.000
248	0.039	0.003	0.006	0.006	0.005	0.001	0.001	0.003
227	0.037	0.000	0.006	0.003	0.004	0.001	0.000	0.001
206	0.042	0.000	0.005	0.003	0.004	0.002	0.002	0.000
185	0.035	0.031	0.006	0.009	0.004	0.003	0.000	0.000
164	0.039	0.031	0.006	0.004	0.005	0.001	0.001	0.002
143	0.038	0.031	0.005	0.004	0.004	0.016	0.000	0.000
122	0.036	0.030	0.004	0.003	0.003	0.001	0.000	0.000
103[(a)]	0.036	0.030	0.004	0.002	0.002	0.000	0.000	0.002
80	0.032	0.024	0.056	0.000	0.000	0.000	0.000	0.000
59	0.029	0.097	0.068	0.065	0.057	0.000	0.000	0.000
38	0.032	0.066	0.078	0.085	0.097	0.030	0.020	0.000
17	0.102	0.095	0.137	0.157	0.175	0.202	0.199	0.234
16	NA[(b)]	NA	NA	NA	NA	0.205	0.207	NA

(a) 101 inches for gamma scans 10, 11, and 12.
(b) NA—no data taken at this elevation.

Table 2.5. Mass Fraction of UDS from Gamma Count, Approach 2, Equation (2.18)

Elevation (in.)	w_S, Gamma Scan Identification # (see App. A, 5/31/00 to 6/2/00)							
	5	6	7	8	9	10	11	12
290	0.013	0.002	0.003	0.001	0.001	0.001	0.000	0.001
269	0.012	0.001	0.002	0.001	0.001	0.000	0.000	0.000
248	0.011	0.001	0.002	0.002	0.001	0.000	0.000	0.001
227	0.011	0.000	0.002	0.001	0.001	0.000	0.000	0.000
206	0.012	0.000	0.002	0.001	0.001	0.001	0.000	0.000
185	0.010	0.009	0.002	0.003	0.001	0.001	0.000	0.000
164	0.011	0.009	0.002	0.001	0.001	0.000	0.000	0.001
143	0.011	0.009	0.001	0.001	0.001	0.005	0.000	0.000
122	0.010	0.009	0.001	0.001	0.001	0.000	0.000	0.000
103[(a)]	0.010	0.009	0.001	0.001	0.001	0.000	0.000	0.001
80	0.009	0.007	0.016	0.000	0.000	0.000	0.000	0.000
59	0.008	0.028	0.020	0.019	0.017	0.000	0.000	0.000
38	0.009	0.019	0.022	0.025	0.028	0.009	0.006	0.000
17	0.030	0.027	0.040	0.045	0.051	0.058	0.058	0.068
16	NA[(b)]	NA	NA	NA	NA	0.059	0.060	NA

(a) 101 inches for gamma scans 10, 11, and 12.
(b) NA—no data taken at this elevation.

The solids concentration data of Table 2.4 and Table 2.5 were converted to UDS mass via trapezoidal integration with elevation as

$$m_{Si} = \Delta z_i A_T \rho_{Bi} w_{Si} \tag{2.19}$$

where Δz_i is the difference in elevation for gamma measurement interval i, and w_{Si} is the average mass fraction in Δz_i. The mass fraction at 290 inches is assumed to extend to the waste surface (329 inches). The bulk density in Δz_i, ρ_{Bi}, is given by

$$\rho_{Bi} = \frac{1}{\frac{w_{Si}}{\rho_S} + \frac{1 - w_{Si}}{\rho_L}} \tag{2.20}$$

It is assumed that the UDS density is constant with elevation.

The UDS mass in Table 2.6 and Table 2.7 represents the UDS mass from the indicated elevation to the next elevation above. It is again apparent that Approach 1 results in significant solids at elevations the URSILLA and grab samples indicated were solids free. Also included in Table 2.6 and Table 2.7 is the summation of the UDS from the lowest gamma measurement elevation, approximately 17 inches. Comparing this sum to the estimated total UDS in the tank, 141,565 kg (Section 2.1.1.1), shows that the results from Approach 1 for gamma scan 5 (profile 1 of Figure 2.3), taken immediately post-mixing, are unphysical. Neglecting any solids that are present below 17 inches (concentration may be reasonably expected to be at least that at 17 inches), the summed UDS mass exceeds the total UDS mass by 14%. Thus, it is conclusively shown that Approach 1 over-predicts the UDS suspension.

The mass fraction of UDS below the bottom gamma measurement elevation resulting from Approach 2 was compared to the mass fraction of UDS in the initial sediment and that of grab-sample 1AZ-00-67. This provided a basis for considering whether Approach 2 under-predicts the UDS suspension for gamma cps greater than those directly associated with the grab-sample concentration data.

The average solids concentration, w_{SA}, below the bottom gamma measurement elevation is given by

$$w_{SA} = \frac{1}{1 + \rho_L \left(\frac{\Delta z A_T}{\Delta m_S} - \frac{1}{\rho_S} \right)} \tag{2.21}$$

where Δz is the lowest gamma measurement elevation, and Δm_S, the mass of UDS below the bottom gamma measurement elevation, is the difference in the estimated total (141,565 kg) and summed UDS mass.

From Section 2.1.1.1, the average solids concentration in the initial sediment was 48% by mass. It is thus reasonable to expect that, allowing for observed radial variation in the concentration of solids on the tank bottom (Carlson et al. 2001), the maximum UDS concentration in the tank will not significantly

exceed this value. Equation (2.21) results are provided in Table 2.8, and all results are reasonable with respect to the initial condition.

Table 2.6. UDS Mass, Approach 1

Elevation (in.)	m_{Si} (kg), Gamma Scan Identification # (see App. A, 5/31/00 to 6/2/00)							
	5	6	7	8	9	10	11	12
290	22074	3023	5923	2146	2106	1798	447	873
269	11403	1049	2437	998	851	491	120	234
248	10782	689	1675	1193	934	182	86	381
227	10429	450	1595	1164	1153	289	85	498
206	10811	0	1485	808	990	437	229	123
185	10497	4149	1512	1687	1001	747	269	0
164	10071	8371	1592	1807	1148	523	136	272
143	10452	8404	1426	1100	1113	2247	96	272
122	10104	8253	1148	969	883	2330	0	0
103[(a)]	8687	7188	979	626	626	178	0	258
80	10299	8173	9095	336	339	0	0	258
59	8286	16699	17161	8849	7792	0	0	0
38	8228	22780	20300	20889	21452	4038	2706	13
17	18562	22453	30415	34500	39100	32979	31075	33288
16	NA[(b)]	NA	NA	NA	NA	2661	2649	NA
Sum	160685	111681	96742	77070	79487	48899	37898	36469

(a) 101 inches for gamma scans 10, 11, and 12.
(b) NA—no data taken at this elevation.

Table 2.7. UDS Mass, Approach 2

Elevation (in.)	m_{Si} (kg), Gamma Scan Identification # (see App. A, 5/31/00 to 6/2/00)							
	5	6	7	8	9	10	11	12
290	6293	873	1708	620	609	520	129	253
269	3253	303	703	289	246	142	35	68
248	3078	199	484	345	270	53	25	110
227	2979	130	461	336	333	84	25	144
206	3086	0	429	234	286	127	66	35
185	2998	1195	437	487	289	216	78	0
164	2878	2397	460	522	332	151	39	79
143	2985	2407	412	318	322	649	28	79
122	2887	2364	332	280	255	672	0	0
103[(a)]	2483	2059	283	181	181	52	0	75
80	2946	2344	2605	97	98	0	0	75
59	2373	4731	4859	2533	2233	0	0	0
38	2357	6404	5725	5886	6041	1163	781	4
17	5246	6315	8467	9556	10767	9152	8644	9234
16	NA[(b)]	NA	NA	NA	NA	713	711	NA
Sum	45843	31721	27365	21684	22263	13693	10560	10155

(a) 101 inches for gamma scans 10, 11, and 12.
(b) NA—no data taken at this elevation.

Table 2.8. Average Mass Fraction of Solids Below Lowest Gamma Measurement Elevation, Equation (2.21). Approach 1.

w_{SA}, Gamma Scan Identification # (see App. A, 5/31/00 to 6/2/00)							
5	6	7	8	9	10	11	12
0.36	0.41	0.42	0.44	0.43	0.48	0.49	0.47

However, the average mass-fraction results of Table 2.8 are not in agreement with grab-sample 1AZ-00-67, which indicated a mass fraction of 0.094 at an elevation of 6 inches at the time of gamma scan 11 (Table 2.2). This comparison, in conjunction with an average concentration equivalent to the initial condition with the UDS mass still above 17 inches, Table 2.7 (initial sediment depth approximately 17.5 inches) suggests that while Approach 1 is appropriate for gamma cps in the range associated with the grab-sample data (Table 2.3), it under-predicts for the higher gamma cps. Alternatively, as the solid-liquid interface approximation from the gamma scans, taken from the midpoint of the high and low gamma readings, is in good agreement with the URSILLA and grab-sample results (Carlson et al. 2001), a more detailed integration scheme for the UDS below the "steps" in the gamma profiles (e.g., Figure 2.3) may provide more equivalent results. Regardless, the Approach 2 results are reasonable within the understanding of the waste conditions, and the results for gamma scan 5, taken immediately post-mixing, are evaluated for UDS suspension with Approach 2.

The gamma cps for gamma-scan 5 from 38 to 290 inches elevation are within the data range. If the initial UDS inventory was homogenously mixed within the tank, the mass fraction of the total UDS above 38 inches would be 0.88. Thus, if the mixer pump operations in AZ-101 homogenously suspended the waste, the UDS mass 38 inches and above estimated from gamma scan 5 should also be 0.88. From Table 2.7, the mass fraction of the total UDS above 38 inches is 0.29, indicating that only 32% of the UDS required for homogenous mixing were suspended. This result is similar to the quantitative analyses reported in Carlson et al. (2001).

The effect of the delay in measurement (gamma readings are immediately post-mixer pump operation) can be investigated by considering differences in results of gamma scans 5 and 6, which are separated in time equivalent to gamma scan 5 and the mixer pump operation. However, the gamma scans are conducted from the waste surface to the bottom, and gamma scan 5 (profile 1 of Figure 2.3) shows constant count with depth, indicating that settling during gamma scan 5 was not significant.[(a)] Further, it is reasonable to expect some period of continued significant fluid motion upon cessation of the mixer pump operation. Thus, investigating the delay effect by comparing gamma scans 5 and 6 is expected to over-estimate the potential impact.

The gamma cps for gamma-scan 6 from 80 to 290 inches elevation are within the data range. Homogenous mixing above 80 inches would result in 0.76 of the initial UDS inventory being suspended therein. The mass fractions of the total UDS above 80 inches for gamma scans 5 and 6 are 0.25 and 0.10, respectively. Therefore the maximum effect of the measurement delay would suggest that 82% of the UDS required for homogenous mixing were suspended.

(a) The radionuclides expected to be indicated by the reported gamma cps include ^{152}Eu and ^{154}Eu (Carlson et al. 2001). The concentration (μCi/g) of ^{154}Eu for the centrifuged solids of grab-samples 1AZ-00-35, 36, and 38 (the only samples with this analysis) is relatively constant (Bell 2001).

The approximate 3.5-hour difference in cessation of mixer pumps 1 and 2 operations potentially influenced the radial distribution of the solids. There is evidence of radial non-homogeneity of UDS on the tank bottom (Carlson et al. 2001). The rotational operation of the mixer pumps may also potentially have influenced the radial distribution of the solids. However, off-bottom radial uniformity is indicated by the very good agreement for the solid-liquid interface from radially distributed instrumentation in five different risers, Section 2.3.1.

Although there are uncertainties in the data (e.g., see discussion on the mass fraction of UDS in the grab samples, Section 2.3.2.1) and the functionality developed from that data (the effect of the fit is expected to be minimized by application within the data region), these uncertainties are not expected to be substantial enough to significantly alter the difference in homogeneity as evaluated. Measurement delays from mixer pump operation and potential radial variation are also not expected to significantly impact the homogeneity difference.

3.0 AY-102 Waste Properties and Tank Configuration

The waste stored in AY-102 consists of a deep liquid layer overlaying a settled solids layer. The total waste depth in AY-102 is approximately 343 inches (TWINS[(a)]). Best-estimate values for current AY-102 waste properties are provided in Section 3.1.1. As with the AZ-101 waste properties, Section 2.1.1, significant digits are not considered, and all values are best-estimate approximations. The tank configuration is summarized in Section 3.1.2.

3.1.1 AY-102 Liquid and Undissolved Solids

The liquid density in AY-102 is approximately 1.17 g/mL (Hu 2007). A representative liquid temperature is approximately 113°F (Hu and Barker 2003), and the dynamic viscosity of AY-102 liquid at that temperature is approximately 3 cP (TWINS data from Attachment B, Warrant 2001; see Onishi and Wells 2004).

The sediment density is approximately 1.55 g/mL (Hu 2007), and the UDS have a bulk density of 2.5 g/mL (Onishi and Wells 2004). With Equations (2.1) and (2.2), the UDS content in the sediment can be estimated at 29% by volume, 46% by mass.

The sediment layer is approximately 64 inches thick (Hu 2007). From Equation (2.3), the UDS mass in the tank is 476,571 kg. The liquid mass is 3,823,922 kg.

3.1.1.1 AY-102 UDS Particulate Characterization

Synonymously with AZ-101, Section 2.1.1.2, the UDS particulate in AY-102 is characterized by a PSDD as per the Case 3 approach of Wells et al. (2007). The presented PSDD is a representation of the AY-102 UDS particulate, and the discrepancy of the UDS density in Section 3.1.1, 2.5 g/mL, and the volume-weighted average from Table 3.1, 3.63 g/mL, is acknowledged.

The AY-102 "minimal disturbance" particle-size distribution was combined with the insoluble solid-phase compounds, volume fractions thereof, and crystal densities (Wells et al. 2007, Table A.3 and Section 3.2). The resulting PSDD is provided in Table 3.1.

The settling velocity of the AY-102 PSDD was computed via Equations (2.4) and (2.5), and the cumulative volume-based probability is presented in Figure 3.1. The 50^{th} (median) and 95^{th} percentiles by volume of settling velocity are approximately 4.6E-6 and 8.8E-4 m/s, respectively.

The estimated *in situ* bulk UDS settling velocity in AY-102 during retrieval of C-106 (approximately 85% of the sediment by volume in AY-102 is from C-106), inferred from the sediment level growth and liquid depth, ranges from 6E-6 to 5E-5 m/s, depending on the retrieval batch (Cuta et al. 2000). These *in situ* settling rates correspond approximately to the 55^{th} to 85^{th} percentile of the PSDD, Figure 3.1. However, the volume-weighted average settling velocity, Equation (2.6), is 3.9E-4 m/s, approximately the 94^{th} percentile of the PSDD. Thus, the volume-weighted average settling velocity exceeds the *in situ* estimates.

(a) TWINS: Tank Waste Information System database. http://twins.pnl.gov/twins3/twins.htm

However, the volume-weighted average comparison may be reasonable. This is similar to the AZ-101 comparison, Section 2.1.1.2, in which the percentile results of the AY-102 settling velocity may imply that the measured particle sizes are biased low. It is again emphasized that, as the PSDDs are intended to be representative and are developed synonymously, the AZ-101 and AY-102 waste characteristics were compared with the PSDDs as presented.

3.1.2 AY-102 Tank Configuration

Tank AY-102 is essentially equivalent to AZ-101, Section 2.12. It is a 37.5-ft-radius 1,406,800-gallon DST with a maximum operating capacity of 1,160,00 gallons (Barker 2003). AY-102 contains ALCs in the same configuration as AZ-101.

Table 3.1. AY-102 PSDD

	Solid Phase Compounds and Density (g/mL)										
	Fe_2O_3	$Al(OH)_3$	$Ca_5OH(PO_4)_3$	MnO_2	$Ni(OH)_2$	$Na_2U_2O_7$	$LaPO_4•2H_2O$	Bi_2O_3	Ag_2CO_3	ZrO_2	PuO_2
	5.24	2.42	3.14	5.026	4.1	5.617	6.51	8.9	6.077	5.68	11.43
Particle Size (μm)	Solid Volume Fraction										
0.22	3.4E-05	5.3E-05	5.3E-06	5.2E-06	1.2E-06	1.0E-06	4.8E-07	2.4E-08	8.6E-09	6.5E-09	3.9E-09
0.28	4.6E-04	7.1E-04	7.2E-05	7.0E-05	1.6E-05	1.4E-05	6.5E-06	3.3E-07	1.2E-07	8.8E-08	5.3E-08
0.36	6.5E-04	1.0E-03	1.0E-04	1.0E-04	2.2E-05	2.0E-05	9.2E-06	4.7E-07	1.7E-07	1.2E-07	7.5E-08
0.46	6.6E-04	1.0E-03	1.0E-04	1.0E-04	2.3E-05	2.0E-05	9.3E-06	4.7E-07	1.7E-07	1.3E-07	7.6E-08
0.6	9.5E-04	1.5E-03	1.5E-04	1.5E-04	3.3E-05	2.8E-05	1.3E-05	6.8E-07	2.4E-07	1.8E-07	1.1E-07
0.77	5.6E-03	8.7E-03	8.7E-04	8.6E-04	1.9E-04	1.7E-04	7.9E-05	4.0E-06	1.4E-06	1.1E-06	6.5E-07
1	2.3E-02	3.5E-02	3.5E-03	3.4E-03	7.7E-04	6.7E-04	3.2E-04	1.6E-05	5.7E-06	4.3E-06	2.6E-06
1.29	3.7E-02	5.7E-02	5.7E-03	5.6E-03	1.3E-03	1.1E-03	5.2E-04	2.6E-05	9.3E-06	7.0E-06	4.2E-06
1.67	3.4E-02	5.2E-02	5.2E-03	5.1E-03	1.2E-03	1.0E-03	4.7E-04	2.4E-05	8.5E-06	6.4E-06	3.9E-06
2.15	3.0E-02	4.7E-02	4.8E-03	4.6E-03	1.0E-03	9.1E-04	4.3E-04	2.2E-05	7.7E-06	5.8E-06	3.5E-06
2.78	3.1E-02	4.9E-02	4.9E-03	4.8E-03	1.1E-03	9.4E-04	4.4E-04	2.3E-05	7.9E-06	6.0E-06	3.6E-06
3.59	2.8E-02	4.4E-02	4.4E-03	4.3E-03	9.6E-04	8.4E-04	4.0E-04	2.0E-05	7.1E-06	5.4E-06	3.2E-06
4.64	2.7E-02	4.2E-02	4.3E-03	4.2E-03	9.4E-04	8.2E-04	3.8E-04	2.0E-05	6.9E-06	5.2E-06	3.1E-06
5.99	2.5E-02	3.8E-02	3.8E-03	3.8E-03	8.5E-04	7.4E-04	3.5E-04	1.8E-05	6.2E-06	4.7E-06	2.8E-06
7.74	2.0E-02	3.2E-02	3.2E-03	3.1E-03	7.0E-04	6.1E-04	2.9E-04	1.5E-05	5.2E-06	3.9E-06	2.4E-06
10	1.7E-02	2.6E-02	2.6E-03	2.6E-03	5.7E-04	5.0E-04	2.4E-04	1.2E-05	4.2E-06	3.2E-06	1.9E-06
12.92	1.6E-02	2.5E-02	2.5E-03	2.5E-03	5.5E-04	4.8E-04	2.3E-04	1.2E-05	4.1E-06	3.1E-06	1.9E-06
16.68	1.5E-02	2.3E-02	2.3E-03	2.3E-03	5.2E-04	4.5E-04	2.1E-04	1.1E-05	3.8E-06	2.9E-06	1.7E-06
21.54	6.4E-03	1.0E-02	1.0E-03	9.8E-04	2.2E-04	1.9E-04	9.1E-05	4.6E-06	1.6E-06	1.2E-06	7.4E-07
27.83	2.0E-03	3.1E-03	3.1E-04	3.0E-04	6.8E-05	5.9E-05	2.8E-05	1.4E-06	5.0E-07	3.8E-07	2.3E-07
35.94	1.1E-03	1.8E-03	1.8E-04	1.7E-04	3.9E-05	3.4E-05	1.6E-05	8.1E-07	2.9E-07	2.2E-07	1.3E-07
46.42	1.4E-03	2.2E-03	2.3E-04	2.2E-04	5.0E-05	4.3E-05	2.0E-05	1.0E-06	3.6E-07	2.8E-07	1.7E-07
59.95	1.7E-03	2.7E-03	2.7E-04	2.6E-04	5.9E-05	5.2E-05	2.4E-05	1.2E-06	4.4E-07	3.3E-07	2.0E-07
77.43	2.3E-03	3.6E-03	3.6E-04	3.6E-04	8.0E-05	7.0E-05	3.3E-05	1.7E-06	5.9E-07	4.4E-07	2.7E-07
100	3.2E-03	5.0E-03	5.0E-04	4.9E-04	1.1E-04	9.5E-05	4.5E-05	2.3E-06	8.0E-07	6.1E-07	3.7E-07
129.15	4.1E-03	6.4E-03	6.4E-04	6.3E-04	1.4E-04	1.2E-04	5.8E-05	3.0E-06	1.0E-06	7.9E-07	4.8E-07
166.81	3.1E-03	4.8E-03	4.8E-04	4.7E-04	1.1E-04	9.2E-05	4.3E-05	2.2E-06	7.8E-07	5.9E-07	3.5E-07
215.44	2.6E-03	4.1E-03	4.1E-04	4.0E-04	8.9E-05	7.8E-05	3.7E-05	1.9E-06	6.6E-07	5.0E-07	3.0E-07
278.26	2.1E-04	3.3E-04	3.3E-05	3.2E-05	7.3E-06	6.4E-06	3.0E-06	1.5E-07	5.4E-08	4.1E-08	2.4E-08
Total Solid-Phase Volume Fraction	0.34	0.53	0.053	0.052	0.012	0.010	0.005	0.0002	0.00009	0.00006	0.00004

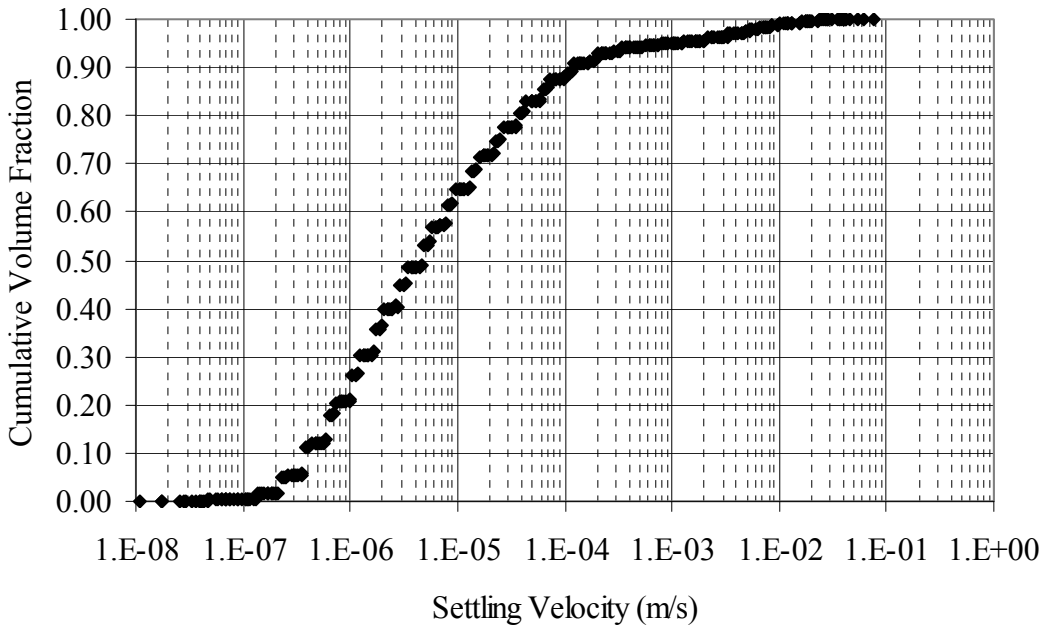

Figure 3.1. Cumulative UDS Volume Fraction as Function of Settling Velocity for AY-102

4.0 Conclusions

The suspension of solids in Hanford DST AZ-101 due to operation of the baseline mixing system has been evaluated, Section 2.3. It is concluded that the mixing in AZ-101 resulted in suspension of 32% of the particulate required for homogenous suspension.

AY-102 is the WTP commissioning feed tank, and the solid suspension therein is considered via the solid suspension performance of the baseline feed delivery mixer pumps in AZ-101. The AZ-101 and AY-102 waste properties and tank configurations were compared, and the implications for solids suspension in AY-102 are discussed in Section 4.1. Estimates for the Hanford waste in general for DST feed staging tanks are made in Section 4.2. Recommendations are provided in Section 4.3 for improving the understanding of solids suspension during mixer pump operation.

4.1 Solid Suspension AY-102

The tank configurations of AZ-101 and AY-102 are equivalent, Sections 2.1.2 and 3.1.2. Thus, any differences in the suspension of solids via equivalent operation of the baseline mixing system are due to differences in the waste properties.

AZ-101 and AY-102 waste properties are reported in Sections 2.1.1 and 3.1.1 respectively. The 4% difference in fill heights in AZ-101 and AY-102 will not influence mixing performance. The UDS particulate was compared with the volume-weighted average settling velocity. The volume-weighted average settling velocity in AZ-101 (4.3E-5 m/s, Section 2.1.1.2) is approximately 10% of that in AY-102 (3.9E-4 m/s, Section 3.1.1.1). It is therefore expected that the quantity of solids suspension in AY-102 for equivalent conditions would be less than that of AZ-101. The anomaly of the *in situ* settling velocity and the PSDD results presented in Sections 2.1.1.2 and 3.1.1.1 may exacerbate the settling velocity difference.

The mixing analysis of AY-102, Onishi and Wells (2004), was focused on the capability of the baseline mixer pumps to mobilize the sediment. As such, the waste properties selected focused on those pertinent to mobilization (i.e., sediment shear strength), and representative values were selected for the remaining properties. The particle-size distribution is taken from the same reference as that of the current analysis (Bechtold 2002), but the outlier particle-size distribution of Bechtold (2002) was excluded from Onishi and Wells (2004). The 99th percentile particle size in the current analysis is thus approximately 167 μm compared to 17 μm in Onishi and Wells. In addition, the solids particulate density in Onishi and Wells (2004) was set at 2.5 g/mL, while in the current analysis, the density ranges from 2.42 to 11.43 g/mL as a function of the fraction of the individual solid phase compounds. As a result, the volume-weighted average settling velocity of Onishi and Wells (2004) is less than 4% that of the current analysis. Once solid particulate was mobilized, it was suspended, and near homogenous suspension was indicated for the sediment that was mobilized.

AY-102 contains approximately 3.4 times as much UDS by mass as AZ-101. Therefore, for the same operating conditions, suspension in AY-102 would be reduced. However, increased solids loading may reduce the particulate settling velocity, so conflicting phenomena with regards to particulate suspension exist. Other complicating phenomenon such as pump performance with increased solids loading may impact mixing performance as well.

The ratio of the hindered particulate settling velocity to free particulate settling velocity is significantly impacted once the solid concentration exceeds approximately 10% by volume (Govier and Aziz 1987). Fully homogenous conditions in AY-102 would result in a solids concentration by volume of approximately 5%.

The hindered settling velocity can be expressed by

$$U_H = U_T\left(1-\frac{\phi}{\phi_{max}}\right)^{4.5} \tag{4.1}$$

where U_T is the free settling velocity (see Equation [2.4]), and ϕ and ϕ_{max} are the local and settled volume fractions, respectively (Wells et al. 2008). Holding the kinematic viscosity of Equation (2.4) constant at the liquid value, the homogenous concentration of 5% reduces the AY-102 particulate volume-weighted average settling velocity such that AZ-101 is 25% that of AY-102. A solids concentration of approximately 11% by volume is required to reduce the volume-weighted average settling velocity of the AY-102 particulate to that of AZ-101.

Comparing the AY-102 and AZ-101 waste properties suggests that the non-homogenous mixing results of AZ-101 imply that AY-102 will not be homogenously mixed by the baseline mixing system. It is likely that less than 32% of the particulate required for homogenous suspension would be achieved.

4.2 Solids Suspension for Hanford Waste

Solids-suspension estimates for the Hanford waste in general in any DST feed staging tank with the baseline mixing system were considered. All Hanford DSTs are essentially equivalent in tank configuration with the exception of the ALCs (Barker 2003). The effect of the ALCs on sediment mobilization and suspension has not been quantified. However, in a computational fluid dynamics analysis of pump jet mixing in AZ-102, Onishi et al. (2000), it was concluded that the ALCs did not have a significant impact on the sediment erosion.

If the influence of the ALCs is assumed to be minimal, the suspension of solids in any feed tank is a function of the waste properties. So long as the solid-liquid interface during mixing is, as in AZ-101, the waste surface, solids suspension will not be a function of the fill height. If it is further assumed that the liquid properties are rendered relatively constant by the dilution process required to prepare the waste for the WTP, then the suspension of the solids will be dependent solely on the particulate properties.

The Case 3 PSDD of Wells et al. (2007) represents the Hanford insoluble solids as a whole, and, as evidenced by the variation to the PSDDs of AZ-101 and AY-102, Sections 2.1.1 and 3.1.1, variability is expected within the feed tanks. The Case 3 PSDD is used for this general qualitative discussion.

The cumulative volume-based probability of the settling velocity of the Case 3 PSDD is presented in Figure 4.1. The 50th (median) and 95th percentiles by volume of settling velocity are approximately 4.6E-5 and 3.8E-3 m/s, respectively. The volume-weighted average settling velocity is 1.4E-3 m/s, approximately 30 and 4 times those of AZ-101 and AY-102, respectively.

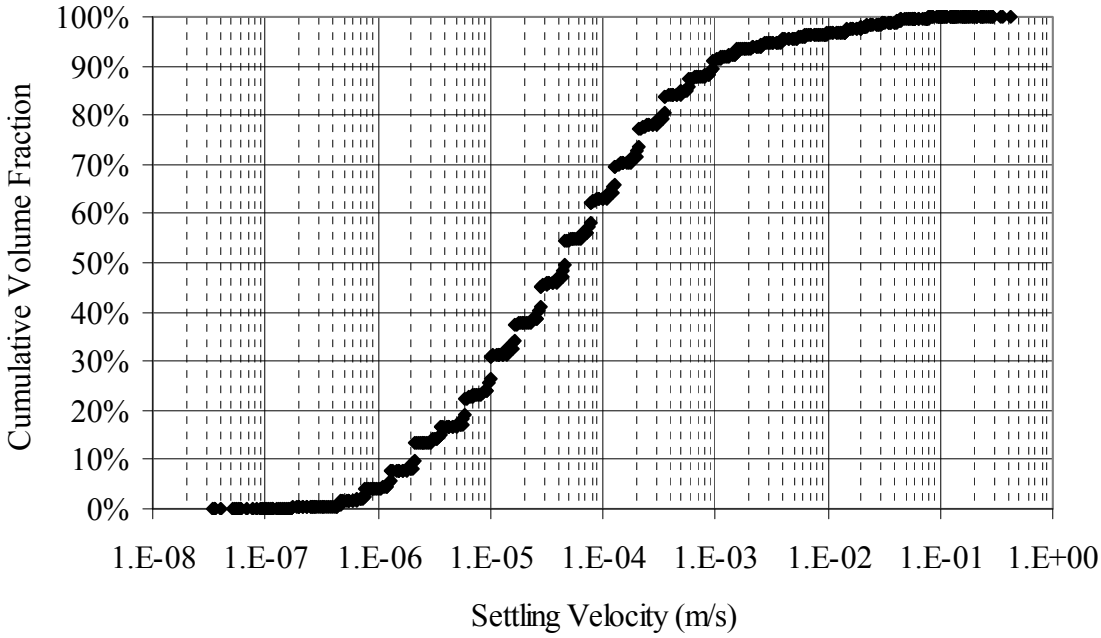

Figure 4.1. Cumulative UDS Volume Fraction as Function of Settling Velocity for Hanford Insoluble Solids, Case 3 PSDD, Wells et al. (2007)

The sediment depths in the DST feed staging tanks may be up to 200 inches. The solid volume fraction in AZ-101, 0.32, can be shown to bound the current Hanford sludge (i.e., insoluble solid) sediment, with typical values at 0.2 to 0.3. Thus, with a sediment 200 inches deep, the solids loading in a DST feed staging tank may exceed that of AZ-101 by approximately 10 times. Fully homogenous conditions in a feed staging tank with 200 inches of sediment at 30% solids by volume and a maximum fill height of 420 inches would result in a solids concentration by volume of approximately 14%. This solids concentration would reduce the volume-weighted average settling velocity of the Hanford insoluble particulate to approximately 2 times that of AZ-101.

The qualitative comparison implies that the baseline mixing system will face significant challenges in DST feed staging tanks with regard to homogenous suspension of the Hanford insoluble solids.

4.3 Recommendations

Recommendations of subject areas that should be focused on, either in the application of existing instrumentation or for new instrumentation, to reduce uncertainties in the homogeneity of mixing include:

- Develop calibrated concentration data for the concentration measurement device over the expected range of concentrations.
- Deploy the concentration measurement device during active mixing.
- Deploy the concentration measurement device over the waste depth. Tank-bottom information is critical.

- Deploy the concentration measurement device at different radial locations.
- Develop concurrent concentration data and sample analysis of *in situ* conditions.
- Operational changes such as waste transfer will affect mixing, and the effects must be evaluated.
- Select mixing demonstration vessels that have waste properties that span or bound solids properties and concentrations.
    - Waste properties must be well characterized.
        - Waste chemistry may significantly impact particulate response to shear and subsequent settling rates.
    - Pump operation parameters must be monitored, controlled, and exercised.
    - The relationship of the solid-liquid interface to the liquid surface level must be similar for different vessels.

The development of a data analysis plan to achieve the desired outcomes before testing is critical. The "Lessons Learned" provided in Carlson et al. (2001) should be reviewed and implemented to the extent possible as part of this process.

5.0 References

Barker SA. 2003. *Determination of Hanford Waste Tank Volumes*. RPP-13019, Rev. 0, CH2M HILL Hanford Group, Inc., Richland, WA.

Bechtold DB, WS Callaway, GA Cooke, JB Duncan, DL Herting, JR Jewett, JC Person, and JM TIngey. 2002. *Particle Property Analyses of High-Level Waste Tank Sludges*. HNF-8862 Rev. 0, Fluor Hanford, Richland, WA.

Bell KE. 2000. *Tank 241-AZ-101 Grab Samples Mixer Pump Test Event 6, Analytical Results for the Final Report*. HNF-6052, Rev 0, Fluor Hanford, Richland, WA.

Bell KE. 2001. *Tank 241-AZ-101 Grab Samples From Mixer Pump Test Events 5, 7, 8, and 9 Analytical Results for the Final Results for the Report*. HNF-6062, Rev 0, Fluor Hanford, Richland, WA.

Callaway WS. 2000. *Results of Retrieval Testing of Sludge from Tank 241-AZ-101*. HNF-7078, Rev. 1, Fluor Hanford, Richland, WA.

Camenen B. 2008. "Simple and General Formula for the Settling Velocity of Particles." *Journal of Hydraulic Engineering - ASCE* 133(2):229-233.

Carlson AB, PJ Certa, TM Hohl, JR Bellomy III, TW Crawford, DC Hedengren, AM Templeton, HS Fisher, SJ Greenwood, DG Douglas, and WJ Ulbright Jr. 2001. *Test Report, 241-AZ-101 Mixer Pump Test*. RPP-6548, Rev. 1, Numatec Hanford Corporation, Richland, WA.

Cuta JM, KG Carothers, DW Damschen, WL Kuhn, JA Lechelt, K Sathyanarayana, and LA Stauffer. 2000. *Review of Waste Retrieval Sluicing System Operations and Data for Tanks 241-C-106 and 241-AY-102*. PNNL-13319, Pacific Northwest National Laboratory, Richland, WA.

Enderlin CW, G Terrones, CJ Bates, BK Hatchell, and B Adkins. 2003. *Recommendations for Advances Design Mixer Pump Operation in Savannah River Site Tank 18F*. PNNL-14443, Pacific Northwest National Laboratory, Richland, WA.

Govier GW, and K Aziz. 1987. *The Flow of Complex Mixtures in Pipes*. ISBN 0-88275-547-1, Robert E Krieger Publishing Company, Inc. Malabar, FL.

Hall MN. 2008. *ICD 19 - Interface Control Document for Waste Feed*. 24590-WTP-ICD-MG-01-019, Rev 4. River Protection Project, Waste Treatment Plant, Richland, WA.

Hu TA. 2007. *Methodology and Calculations for the Assignment of Waste Groups for the Large Underground Waste Storage Tanks at the Hanford Site*. RPP-10006, Rev. 6., CH2M HILL Hanford Group, Inc., Richland, WA.

Hu TA, and SA Barker. 2003. *Steady-State Flammable Gas Release Rate Calculation and Lower Flammability Level Evaluation for Hanford Tank Waste*. RPP-5926, Rev. 2A, CH2M HILL Hanford Group, Inc., Richland, WA.

Knoll GF. 2000. *Radiation Detection and Measurement*. ISBN 0-471-07338-5, John Wiley and Sons, Inc., Hoboken, NJ.

Onishi Y, and BE Wells. 2004. *Feasibility Study on Using Two Mixer Pumps for Tank 241-AY-102 Waste Mixing*. PNNL-14763, Pacific Northwest National Laboratory, Richland, WA.

Onishi Y, KP Recknagle, and BE Wells. 2000. *Pump Jet Mixing and Pipeline Transfer Assessment for High-Activity Radioactive Wastes in Hanford Tank 241-AZ-102*. PNNL-13275, Pacific Northwest National Laboratory, Richland, WA.

Onishi Y, BE Wells, SA Hartley, and SK Cooley. 2002. *Pipeline Cross-Site Transfer Assessment for Tank 241-SY-101*. PNNL-13650, Pacific Northwest National Laboratory, Richland, WA.

Stewart CW, MS Fountain, JL Huckaby, LA Mahoney, PA Meyer, and BE Wells. 2005. *Effects of Globally Waste-Disturbing Activities on Gas Generation, Retention, and Release in Hanford Waste Tanks*. PNNL-13781, Rev. 3, Pacific Northwest National Laboratory, Richland, WA.

Warrant RW. 2001. *Results of Retrieval Testing of Sludge from Tank 241-AY-102*. RPP-8909, Rev 0, Fluor Hanford, Richland, WA.

Wells BE, MA Knight, EC Buck, SK Cooley, RC Daniel, LA Mahoney, PA Meyer, AP Poloski, JM Tingey, WS Callaway III, GA Cooke, ME Johnson, MG Thien, DJ Washenfelder, JJ Davis, MN Hall, GL Smith, SL Thomson, and Y Onishi. 2007. *Estimate of Hanford Waste Insoluble Solid Particle Size and Density Distribution*. PNWD-3824, WTP-RPT-153, Rev. 0, Battelle—Pacific Northwest Division, Richland, WA.

Wells BE, KI Johnson, DR Rector, and DS Trent. 2008. *S-102 Transfer Pump Restriction Modeling Results*. PNNL-17424, Pacific Northwest National Laboratory, Richland, WA.

Appendix A

Gamma-Monitoring System Data

Appendix A: Gamma-Monitoring System Data

The gamma-monitoring system data of Figure 2.3, Section 2.3.2.1, and additional data of interest are listed in Table A.1.

Table A.1. Gamma-Monitoring System Data

Figure 2.3 Profile Number [Identification #]	Data File	Date	Time[a]	Height in Vessel (in.)	Gross Rate (cps) [Counts/Live Time]
NA[b] [1]	15F—Above 850 keV Depth Profile—04 27 2000.xls	4/27/00	14:46–15:30	290	36.467
				269	34.800
				248	34.511
				227	34.367
				206	35.511
				185	35.300
				164	33.822
				143	34.389
				122	33.733
				101	33.642
				80	33.289
				68	32.311
				56	34.822
				44	47.056
NA [2]	15C—Above 850 keV Depth Profile—04 30 2000(1).xls	4/30/00	3:04–3:51	290	38.156
				269	35.344
				248	35.289
				227	34.222
				206	34.989
				185	34.556
				164	35.089
				143	35.389
				122	35.100
				101	35.489
				80	35.422
				59	29.979
				38	31.389
				17	230.023
				16	300.267
NA [3]	15C—Above 850 keV Depth Profile—04 30 2000(2).xls		4:57–5:45	290	35.367
				269	33.278
				248	34.678
				227	33.544
				206	35.089
				185	32.622
				164	35.811

Table A.1 (contd)

Figure 2.3 Profile Number [Identification #]	Data File	Date	Time[(a)]	Height in Vessel (in.)	Gross Rate (cps) [Counts/Live Time]
				122	34.044
				101	35.581
				80	34.333
				59	32.456
				38	31.011
				17	232.544
				16	286.278
NA [4]	15C—Above 850 keV Depth Profile—04 30 2000(3).xls		16:34–17:16	290	36.567
				269	32.944
				248	36.653
				227	33.500
				206	34.133
				185	32.844
				164	35.644
				143	37.259
				122	34.200
				101	33.933
				80	34.433
				59	31.367
				38	33.344
				17	245.000
				16	299.956
1 [5]	15C—Above 850 keV Depth Profile—05 31 2000(1).xls	5/31/00	16:31:02	290	51.278
			16:34:36	269	49.444
			16:38:05	248	48.789
			16:41:34	227	48.027
			16:43:51	206	50.322
			16:47:19	185	46.767
			16:50:55	164	48.611
			16:54:25	143	48.300
			16:58:00	122	47.211
			17:01:32	103	47.110
			17:03:55	80	44.933
			17:07:28	59	43.244
			17:10:54	38	44.700
			17:14:18	17	84.300
2 [6]	15C—Above 850 keV Depth Profile—05 31 2000(2).xls		17:44:27	290	30.444
			17:47:50	269	28.058
			17:50:03	248	28.944
			17:53:21	227	26.722
			17:57:04	206	21.811
			18:00:15	185	44.244
			18:03:34	164	44.278
			18:07:08	143	44.378

Table A.1 (contd)

Figure 2.3 Profile Number [Identification #]	Data File	Date	Time[(a)]	Height in Vessel (in.)	Gross Rate (cps) [Counts/Live Time]
			18:10:27	122	43.667
			18:13:54	103	43.822
			18:17:19	80	40.500
			18:20:45	59	81.211
			18:24:32	38	64.111
			18:27:56	17	79.956
3 [7]	15C—Above 850 keV Depth Profile—05 31 2000(3).xls		19:45:56	290	33.667
			19:47:10	269	30.589
			19:50:45	248	30.511
			19:54:06	227	30.256
			19:57:28	206	30.056
			20:00:49	185	30.367
			20:04:09	164	30.389
			20:07:32	143	29.678
			20:10:53	122	29.233
			20:14:21	103	29.500
			20:17:52	80	58.178
			20:21:21	59	65.344
			20:24:50	38	70.411
			20:28:17	17	103.844
4 [8]	15C—Above 850 keV Depth Profile—05 31 2000(4).xls		21:11:01	290	29.467
			21:14:26	269	28.822
			21:17:46	248	30.278
			21:21:08	227	28.700
			21:24:23	206	28.800
			21:27:54	185	32.348
			21:29:12	164	29.300
			21:32:45	143	29.411
			21:36:17	122	28.756
			21:39:34	103	28.322
			21:43:01	80	25.222
			21:46:30	59	63.389
			21:49:53	38	74.644
			21:53:18	17	114.778
5 [9]	15C—Above 850 keV Depth Profile—05 31 2000(5).xls		22:41:07	290	29.422
			22:44:41	269	28.256
			22:48:14	248	29.767
			22:51:38	227	29.167
			22:54:55	206	29.089
			22:58:18	185	29.211
			23:01:41	164	29.700
			23:05:07	143	29.067
			23:08:32	122	28.743
			23:11:28	103	28.333

Table A.1 (contd)

Figure 2.3 Profile Number [Identification #]	Data File	Date	Time[(a)]	Height in Vessel (in.)	Gross Rate (cps) [Counts/Live Time]
			23:14:58	80	25.400
			23:18:24	59	59.111
			23:21:51	38	81.100
			23:25:20	17	125.144
NA [10]	15C—Above 850 keV Depth Profile—06 01 2000(10).xls	6/1/00	15:13	290	29.078
			15:16	269	27.100
			15:20	248	27.789
			15:23	227	27.556
			15:27	206	28.400
			15:30	185	28.844
			15:34	164	27.467
			15:38	143	36.000
			15:41	122	27.811
			15:45	101	26.744
			15:48	80	24.789
			15:52	59	24.267
			15:55	38	43.789
			15:59	17	140.011
			16:02	16	141.900
NA [11]	15C—Above 850 keV Depth Profile—06 01 2000(11).xls		16:40	290	27.567
			16:43	269	26.833
			16:47	248	27.422
			16:50	227	26.500
			16:54	206	28.022
			16:57	185	27.233
			17:01	164	27.467
			17:05	143	26.789
			17:08	122	25.511
			17:12	101	27.034
			17:15	80	24.156
			17:19	59	23.311
			17:22	38	38.300
			17:26	17	138.422
			17:29	16	142.611
6 [12]	15C—Above 850 keV Depth Profile—06 02 2000(9).xls	6/2/00	12:27	290	28.044
			12:30	269	27.067
			12:34	248	28.644
			12:37	227	27.578
			12:41	206	26.644
			12:44	185	26.544
			12:48	164	28.200
			12:52	143	26.133
			12:55	122	26.844
			12:59	101	28.141

Table A.1 (contd)

Figure 2.3 Profile Number [Identification #]	Data File	Date	Time[(a)]	Height in Vessel (in.)	Gross Rate (cps) [Counts/Live Time]
			13:02	80	23.795
			13:06	59	23.400
			13:09	38	27.122
			13:13	17	157.822
			13:16	15	160.856

(a) 5/31/00 times from file 15C—A-000531(1)—80 Spectra.xls. 6/1 and 6/2/00 times inferred from start times listed in Appendix B Master Timeline.xls of Carlson et al. (2001) and time intervals of 15C—A-000531(1)—80 Spectra.xls.
(b) Not applicable.

Carlson AB, PJ Certa, TM Hohl, JR Bellomy III, TW Crawford, DC Hedengren, AM Templeton, HS Fisher, SJ Greenwood, DG Douglas, and WJ Ulbright Jr. 2001. *Test Report, 241-AZ-101 Mixer Pump Test*. RPP-6548, Rev. 1, Numatec Hanford Corporation, Richland, WA.

Distribution

No. of Copies

OFFSITE

No. of Copies

ONSITE

3 WRPS

M. Thien	H6-03
D.H. Shuford	H6-03
D.J. Washenfelder	R2-58

1 ORP

J-S Shuen	H6-60

7 Pacific Northwest National Laboratory

J. M. Cuta	K7-15
J. A. Fort	K7-15
P. A. Gauglitz	K9-75
J. J. Ressler	K5-25
P. A. Scott	K7-15
B. E. Wells (2)	K7-15